Research Article

Dynamic Response of Parallel Hoisting System under Drive Deviation between Ropes with Time-Varying Length

Guohua Cao,[1,2] Xiang Cai,[1,2] Naige Wang,[1,2] Weihong Peng,[3] and Jishun Li[4]

[1]*School of Mechatronic Engineering, China University of Mining and Technology, Xuzhou 221116, China*
[2]*Jiangsu Key Laboratory of Mine Mechanical and Electrical Equipment, China University of Mining and Technology, Xuzhou 221116, China*
[3]*School of Mechanics and Civil Engineering, China University of Mining and Technology, Xuzhou 221116, China*
[4]*State Key Laboratory of Heavy Mining Equipment, Luoyang 471039, China*

Correspondence should be addressed to Guohua Cao; caoguohua@cumt.edu.cn

The dynamic responses of parallel hoisting system with time-varying length and rigid guidance under drive deviation are investigated considering tension and torsion characteristics of the ropes. The variable-domain three-node elements of rope are employed and the corresponding differential algebraic equations (DAEs) are derived using Lagrange's equations of the first kind. The slack situation of the rope is considered, and the dynamic equations which are systems of DAEs are transformed to ordinary differential equations (ODEs). The dynamic responses of tension, torsion, and acceleration are analyzed considering radius' error of the drums, which indicates that the drive deviation between ropes can cause large influence on the tension difference and even cause one of the ropes to slack. However, the torsion of the corresponding rope is active. And unreasonable discordance between ropes should be controlled for the design and manufacture of drum on super deep parallel hoisting system.

1. Introduction

Parallel hoisting system, which has the advantage of large carrying capacity, small rotation of conveyance, excellent security performance, and fine economic performance, works at the manner that one conveyance is hoisted cooperatively by several cables [1]. Parallel hoisting system is widely used due to the increase of lifting heavy and large volume loads, such as elevator hoisting system (Figure 1(a)), mine hoisting system (Figure 1(b)), and parallel suspension platform of vertical shaft in construction.

The parallel hoisting system will vibrate subject to the excitation sources including ripple of the motor, turbulence of transmission device, abrasion of winding drum, and the eccentricity of head sheave. These vibrations will affect the stability of the conveyance and may also cause damage to the ropes, which will further lead to accidents.

Dynamic characteristics of single rope hoisting system with time-varying length have been studied by many

researchers. Zhu and Ni investigated the linear lateral dynamics of beam and string with an arbitrarily varying length by Hamilton's principle and Galerkin's method [2]. Kaczmarczyk and Ostachowicz described the coupled lateral–longitudinal dynamic response of the cables in deep mine hoisting system with a depth of 2085 m and formulated a discrete mathematical model by Rayleigh–Ritz procedure [3]. Wang et al. investigated the lateral response of the moving hoisting conveyance in cable-guided hoisting system [4]. All of these researches in hoisting system with single cable are the foundations for the dynamic research of parallel hoisting system.

As the application of parallel hoisting systems is increasing, people are paying more and more attention on its research. Zhu and Ren developed a spatial discretization and substructure method to accurately calculate the dynamic responses of single and multiple suspension cables with length-variant distributed-parameter components, which
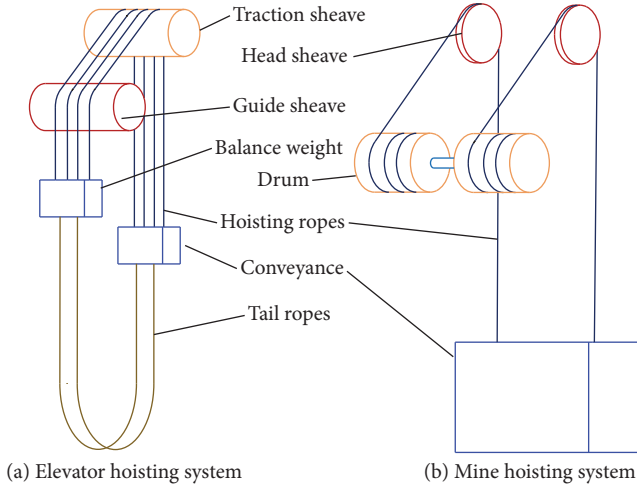
(a) Elevator hoisting system

(b) Mine hoisting system

FIGURE 1: Parallel hoisting system.

FIGURE 2: Model of parallel hoisting system.

simplified the handle of boundary conditions [5]. References [6–9] investigated the dynamics of cable-suspended parallel system, but the vibrations of cables themselves are not considered. So, it could not get accurate results. Shao et al. investigated the dynamics of a sinking winch mechanism in the framework of nonsmooth dynamics considering the unilateral property of cable and presented a numerical simulation method which is suitable for the dynamic analysis of the sinking winch mechanism [10]. Du et al. addressed the dynamic modeling of large CDPMs using a variable-domain finite element method; the effects of cable length variation and the resulting mass variation are also considered [1]. Wang et al. established the longitudinal vibration model of parallel hoisting system with tension autobalance device attached to the ends of all hoisting ropes and showed the influence on longitudinal response of different coefficients and excitations [11].

Finite element method (FEM), as a well-known and efficient numerical method, has been widely used in engineering problems [12]. It can be used to deal with the dynamic problem of continuum [13]. Stylianou and Tabarrok analyzed the dynamic characteristic of an axially moving beam [14, 15]. Wang et al. investigated three-dimensional vibrations of an underwater geometrically nonlinear cable with a weight at the lower end [16]. Moustafa et al. considered the modeling problem of the dynamics of overhead cranes with flexible cable and load hoisting or lowering during crane travel [17]. All these researches are investigated by variable-domain FEM (Vd-FEM). The Vd-FEM does not need to find trial functions to satisfy the boundary conditions while shape functions are used as interpolation functions. And the displacement boundary conditions at upper ends of cables can be satisfied accurately by modifying the global matrix properly.

Wire rope, for its complex helical structure, will produce twist motion or torsion under axial load. Costello derived the coupled stiffness coefficient of wire rope, which can be used to express the relation between axial force and torsion with strain [18]. Thus, when ropes vibrate longitudinally, the torsional vibrations will also occurred. The different upper ends
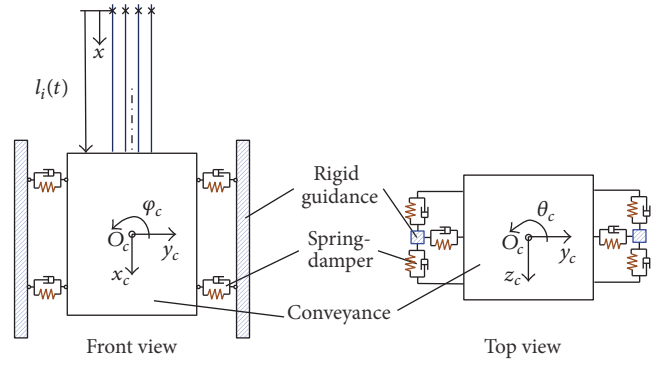
excitations will cause different tension and torsion of ropes. The torsion difference will cause the conveyance rotating around the vertical axis, and tension difference in ropes also causes the conveyance rotating around the horizontal axis. Sometimes the rotation of conveyance can be uncomfortable for the passengers or even damage the guide devices. In this paper, the dynamic responses of parallel hoisting system with time-varying length and rigid guidance under drive deviation are investigated considering tension and torsion characteristics of ropes. The variable-domain three-node elements of rope are used and the corresponding differential algebraic equations (DAEs) are derived by Lagrange's equations of the first kind, which are for working out several challenging problems including the tensions and torsions between the conveyance and cables and the conveyance motion. The dynamic responses of parallel hoisting system are discussed by considering radius' error of drum.

2. Model for Parallel Hoisting System

2.1. Description of Parallel Hoisting System. Parallel hoisting system depicted in Figure 1 can be simplified as k parallel ropes with an attached conveyance which is restrained by rigid guidance, where k is the number of hoisting ropes, as shown in Figure 2. Length of each rope is $l(t)$ at time t excluding the excitation at upper end. The vertically translating velocity and acceleration of ropes are $v(t) = \dot{l}(t)$ and $a(t) = \ddot{l}(t)$, where the overdot denotes time differentiation, and the same representation is used as follows.

$e_i(t)$ represents the longitudinal drive deviation on ith rope at upper end, which might be caused by the radius' error or irregular outline of drum. θ_c and φ_c denote the angle displacements of conveyance about vertical axis x_c and horizontal axis z_c as shown in Figure 2. The following assumptions constrain the analysis. (1) Guidance devices are always keeping in touch with rigid guidance under preload; (2) the whole friction can be neglected; (3) the influence of lateral vibration of rope on the system is small enough to be neglected; (4) the ropes' mechanical parameters remain constant.

2.2. Equations of Motion. The kinetic energy of the k ropes and conveyance is given by
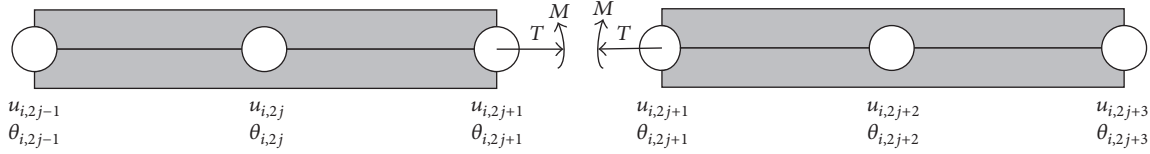
FIGURE 3: Three-node element of rope.

$$T = \sum_{i=1}^{k} \sum_{j=1}^{n} \frac{1}{2} \int_{(j-1)l(t)/n}^{jl(t)/n} \rho \left(\frac{Du_i}{Dt} + v \right)^2 dx$$

$$+ \sum_{i=1}^{k} \sum_{j=1}^{n} \frac{1}{2} \int_{(j-1)l(t)/n}^{jl(t)/n} J \left(\frac{D\theta_i}{Dt} \right)^2 dx \qquad (1)$$

$$+ \frac{1}{2} m_c \left(\dot{u}_c + v \right)^2 + \frac{1}{2} J_{cx} \dot{\theta}_c^2 + \frac{1}{2} J_{cz} \dot{\varphi}_c^2,$$

where n is the number of elements in each rope, ρ is density of hoisting rope per unit length, J is the moment of inertia of hoisting rope about its central axis, and j denotes the jth element of the ropes. m_c, J_{cx}, and J_{cz} are mass and the moment of inertia about its vertical and horizontal axis of conveyance, respectively. u_c is the dynamic longitudinal displacement of conveyance. The operator D/Dt is given by $D/Dt = \partial/\partial t + v(\partial/\partial x)$.

In (1), u_i and θ_i are given as

$$u_i (x, t) = \mathbf{N}_j (x, l(t)) \, \mathbf{q}_{i,j} (t),$$

$$\theta_i (x, t) = \mathbf{N}_j (x, l(t)) \, \mathbf{p}_{i,j} (t), \qquad (2)$$

$$x_j \le x \le x_{j+1}, \quad j = 1, 2, \ldots, n,$$

where $\mathbf{q}_{i,j}(t) = [u_{i,2j-1} \ u_{i,2j} \ u_{i,2j+1}]^{\mathrm{T}}$ and $\mathbf{p}_{i,j}(t) = [\theta_{i,2j-1} \ \theta_{i,2j} \ \theta_{i,2j+1}]^{\mathrm{T}}$ are longitudinal and torsional displacement vectors, $\mathbf{N}_j(x, l) = [N_{j1} \ N_{j2} \ N_{j3}]$ is shape function matrix depending on $l(t)$, where $N_{j1} = 2j^2 - j + nx(1-4j)/l + 2(nx/l)^2$, $N_{j2} = 4[j - j^2 + nx(2j-1)/l - (nx/l)^2]$, and $N_{j3} = 1 - 3j + 2j^2 + nx(3 - 4j)/l + 2(nx/l)^2$.

The jth and $(j + 1)$th elements of ith rope are shown in Figure 3, in which T and M are the tension and torsion between the two elements.

Considering the dynamic displacement and static elastic deformation, the strain energy of the hoisting system is formulated as

$$E_e$$

$$= \sum_{i=1}^{k} \sum_{j=1}^{n} \int_{(j-1)l(t)/n}^{jl(t)/n} \left[\left(T_i^c + \frac{1}{2} T_i^d \right) \varepsilon_i + \left(M_i^c + \frac{1}{2} M_i^d \right) \phi_i \right] dx \qquad (3)$$

$$+ 8 \cdot \frac{1}{2} k_c \left(r_1 \theta_c \right)^2 + 4 \cdot \frac{1}{2} k_c \left(r_2 \varphi_c \right)^2,$$

where $\varepsilon_i = u_{i,x}$ and $\phi_i = \theta_{i,x}$ denote the longitudinal and torsional strain, respectively, where the subscript x denotes partial differentiation with respect to x, and the

same representation is used as follows. The static tension and torsion in ith rope can be expressed as

$$T_i^c = \rho \left(l(t) - x \right) g + \frac{m_c g}{k}, \qquad (4)$$

$$M_i^c = \frac{T_i^c Q_i^c}{Q_i^a}. \qquad (5)$$

The dynamic tension and torsion can be given, respectively, as

$$T_i^d = Q_i^a \varepsilon_i + Q_i^b \phi_i, \qquad (6)$$

$$M_i^d = Q_i^c \varepsilon_i + Q_i^d \phi_i \qquad (7)$$

in which Q_i^a and Q_i^d denote longitudinal and torsional stiffness coefficients of ith rope, respectively. Q_i^b and Q_i^c denote the coupled stiffness coefficient [18]. k_c is the equivalent stiffness of guide devices; r_1 is the horizontal distance between the center of conveyance and rigid guidance; r_2 is the vertical distance between guide devices and the center of conveyance.

Setting the initial position as the place of zero gravitational potential energy, the gravitational potential energy of system can be written as

$$E_g = -\sum_{i=1}^{k} \sum_{j=1}^{n} \int_{(j-1)l(t)/n}^{jl(t)/n} \rho g u_i dx - m_c g u_c. \qquad (8)$$

According to the viscoelastic properties of wire rope [19], the equivalent external nodal load on the jth element of ith rope is formulated as

$$\mathbf{f}_{euj} = \int_{(j-1)l(t)/n}^{jl(t)/n} f_{uc} \mathbf{N}_j^T dx,$$

$$\mathbf{f}_{e\theta j} = \int_{(j-1)l(t)/n}^{jl(t)/n} f_{\theta c} \mathbf{N}_j^T dx, \qquad (9)$$

where $f_{uc} = \zeta_u(Q_i^a \varepsilon_{i,t} + Q_i^b \phi_{i,t})$, $f_{\theta c} = \zeta_\theta(Q_i^c \varepsilon_{i,t} + Q_i^d \phi_{i,t})$, and ζ_u and ζ_θ are longitudinal and torsional damping coefficients, respectively.

The global equivalent external nodal load can be obtained as $\sum \mathbf{f}_{euj}$ and $\sum \mathbf{f}_{e\theta j}$, where $\sum$ denotes the assembly operator of the Vd-FEM.

The damping force of guide device on conveyance is given as

$$F_{e\theta c} = -8c_c r_1 \dot{\theta}_c,$$

$$F_{e\varphi c} = -4c_c r_2 \dot{\varphi}_c, \qquad (10)$$

where c_c is equivalent damping of guide devices.

Since φ_c is very small, it can be obtained approximately by the dynamic displacement of the lower ends of ropes as

$$g_1 = \varphi_c - \frac{(u_{1,2n+1} - u_{2,2n+1})}{d} = 0, \tag{11}$$

where d is the distance between adjacent ropes.

The geometric relationships between dynamic longitudinal displacement of conveyance and k ropes at lower ends are given as

$$g_2 = u_c - \left(u_{1,2n+1} - \frac{d\varphi_c\,(k-1)}{2}\right) = 0,$$
$$g_i = u_{i,2n+1} - (u_{1,2n+1} - (i-1)\,d\varphi_c) = 0, \tag{12}$$
$$i = 3, 4, \ldots, k.$$

The dynamic torsional displacements of lower ends of ropes can be expressed by the rotation angle of conveyance as

$$g_{k+i} = \theta_{i,2n+1} - \theta_c = 0, \quad i = 1, 2, \ldots, k. \tag{13}$$

Substituting (1)–(10) into Lagrange's equations of the first kind [20]

$$\frac{d}{dt}\frac{\partial T}{\partial \dot{Q}_i} - \frac{\partial T}{\partial Q_i} + \frac{\partial\left(E_e + E_g\right)}{\partial Q_i} = F_{ei} + \sum_{j=1}^{2k} \lambda_j \frac{\partial g_j}{\partial Q_i} \tag{14}$$

and using a standard assembly procedure of the FEM [12], the dynamic equations of k ropes and conveyance without the excitations at upper ends can be obtained as

$$\mathbf{M\ddot{Q}} + \mathbf{C\dot{Q}} + \mathbf{KQ} = \mathbf{F} + \mathbf{G}^T \lambda, \tag{15}$$

$$\mathbf{g}\left(\mathbf{Q}, t\right) = \mathbf{0} \tag{16}$$

which is a system of DAEs, where $\mathbf{Q} = [u_{1,1}, \theta_{1,1}, u_{2,1}, \theta_{2,1}, \ldots, u_{k,2n+1}, \theta_{k,2n+1}, u_c, \theta_c, \varphi_c]^T$ is the displacement vector of all the nodes on k ropes and three degrees of freedom of conveyance. $\mathbf{M} = \begin{bmatrix} \mathbf{M}_D & \\ & \mathbf{M}_c \end{bmatrix}$, $\mathbf{C} = \begin{bmatrix} \mathbf{C}_D & \\ & \mathbf{C}_c \end{bmatrix}$, $\mathbf{K} = \begin{bmatrix} \mathbf{K}_D & \\ & \mathbf{K}_c \end{bmatrix}$, and $\mathbf{F} = [\mathbf{F}_D^T \quad \mathbf{F}_c^T]^T$ are the matrixes of mass, damping, stiffness, and force. $\mathbf{M}_D$, $\mathbf{C}_D$, $\mathbf{K}_D$, and $\mathbf{F}_D$ are the global matrixes of ropes assembled from element matrixes, which are listed in the Appendix. And $\mathbf{M}_c = \text{diag}\,(m_c, J_{cx}, J_{cz})$, $\mathbf{C}_c = \text{diag}(0, 8c_c r_1^2, 4c_c r_2^2)$, $\mathbf{K}_c = \text{diag}(0, 8k_c r_1^2, 4k_c r_2^2)$, and $\mathbf{F}_c = [m_c(g-a) \quad 0 \quad 0]^T$. $\mathbf{g}(\mathbf{Q}, t)$ is a $2k$-order vector which includes the constraint equations (11)–(13); $\mathbf{G} = \partial \mathbf{g}/\partial \mathbf{Q}$, $\lambda = [\lambda_1 \quad \lambda_2 \quad \cdots \quad \lambda_{2k}]^T$ are Lagrange multipliers.

Considering the following DAEs calculation, according to (11)–(13), the $2k \times [2k(2n+1) + 3]$ matrix $\mathbf{G}$ can be written as $\mathbf{G} = [\mathbf{G}_0 \quad \mathbf{G}_1]$, where $\mathbf{G}_0$ is $2k \times (4nk+3)$ matrix and $\mathbf{G}_1$ is $2k \times 2k$ matrix.

Rewriting the displacement vector as $\mathbf{Q} = \begin{bmatrix} \mathbf{Q}_0^T & \mathbf{Q}_1^T \end{bmatrix}^T$, where $\mathbf{Q}_0$ is a $4nk+3$ vector and $\mathbf{Q}_1$ is a $2k$ vector, hence, $\mathbf{Q}$ can be expressed by $\mathbf{Q}_0$ as

$$\mathbf{Q} = \mathbf{U}\mathbf{Q}_0, \tag{17}$$

where $\mathbf{U} = \begin{bmatrix} \mathbf{I} \\ -\mathbf{G}_1^{-1}\mathbf{G}_0 \end{bmatrix}$ and $\mathbf{I}$ is $4nk+3$ identity matrix.

Differentiating (17) twice with respect to t yields

$$\dot{\mathbf{Q}} = \mathbf{U}\dot{\mathbf{Q}}_0,$$
$$\ddot{\mathbf{Q}} = \mathbf{U}\ddot{\mathbf{Q}}_0. \tag{18}$$

Substituting (17) and (18) into (15) and premultiplying it by $\mathbf{U}^T$, the dynamic equations of ropes and conveyance without excitations at upper ends are formulated as

$$\widetilde{\mathbf{M}}\ddot{\mathbf{Q}}_0 + \widetilde{\mathbf{C}}\dot{\mathbf{Q}}_0 + \widetilde{\mathbf{K}}\mathbf{Q}_0 = \widetilde{\mathbf{F}}, \tag{19}$$

which is a system of ordinary differential equations (ODEs), where $\widetilde{\mathbf{M}} = \mathbf{U}^T\mathbf{M}\mathbf{U}$, $\widetilde{\mathbf{C}} = \mathbf{U}^T\mathbf{C}\mathbf{U}$, $\widetilde{\mathbf{K}} = \mathbf{U}^T\mathbf{K}\mathbf{U}$, and $\widetilde{\mathbf{F}} = \mathbf{U}^T\mathbf{F}$.

When longitudinal excitations $u_{i,1} = e_i(t)$ and torsional constraint $\theta_{i,1} = 0$ are imposed on the upper ends of ropes, the dynamic equations should be converted into the form as follows:

$$\overline{\mathbf{M}}\,\ddot{\overline{\mathbf{Q}}}_0 + \overline{\mathbf{C}}\,\dot{\overline{\mathbf{Q}}}_0 + \overline{\mathbf{K}}\,\overline{\mathbf{Q}}_0 = \overline{\mathbf{F}}, \tag{20}$$

where $\overline{\mathbf{M}}$, $\overline{\mathbf{C}}$, and $\overline{\mathbf{K}}$ are obtained from $\widetilde{\mathbf{M}}$, $\widetilde{\mathbf{C}}$, and $\widetilde{\mathbf{K}}$ by deleting the 1 to $2k$ rows and the 1 to $2k$ columns and $\overline{\mathbf{Q}}_0$ is obtained from $\mathbf{Q}_0$ by deleting the 1 to $2k$ row. And $\overline{\mathbf{F}}$ is obtained form $\widetilde{\mathbf{F}}$ by the operation that

$$\overline{\mathbf{F}}_a = \widetilde{\mathbf{F}}_{a+2k} - \sum_{p=1}^{k} \widetilde{\mathbf{M}}_{a+2k,2p-1}\ddot{e}_p\,(t) - \sum_{p=1}^{k} \widetilde{\mathbf{C}}_{a+2k,2p-1}\dot{e}_p\,(t)$$
$$- \sum_{p=1}^{k} \widetilde{\mathbf{K}}_{a+2k,2p-1}e_p\,(t), \tag{21}$$

where $a = 1, 2, \ldots, 4nk + 3 - 2k$.

2.3. Rope Slack Condition. Now consider a conveyance hoisted by two ropes, the dynamics of the system will be more complex if one of ropes is slack due to the deviation of drums. One rope is completely slack or tight which is judged by the tension at the connection point of the conveyance. Before the rope is completely slack, the dynamic response can be obtained by the equations derived before. But, if the slack rope is completely slack, the constraint condition between ropes and conveyance will change.

When one rope is slack, it will not bear loads from the conveyance while the torsion still exists. Then, the dynamic torsional displacements of lower ends of ropes can be expressed by the rotation angle of conveyance as

$$g_i = \theta_{i,2n+1} - \theta_c = 0, \quad i = 1, 2. \tag{22}$$

If rope 1 was slack, the relationship between dynamic longitudinal displacement of conveyance and ropes at lower ends can be given as

$$g_3 = \varphi_c + \frac{2}{d}\left(u_{2,2n+1} - u_c\right) = 0. \tag{23}$$
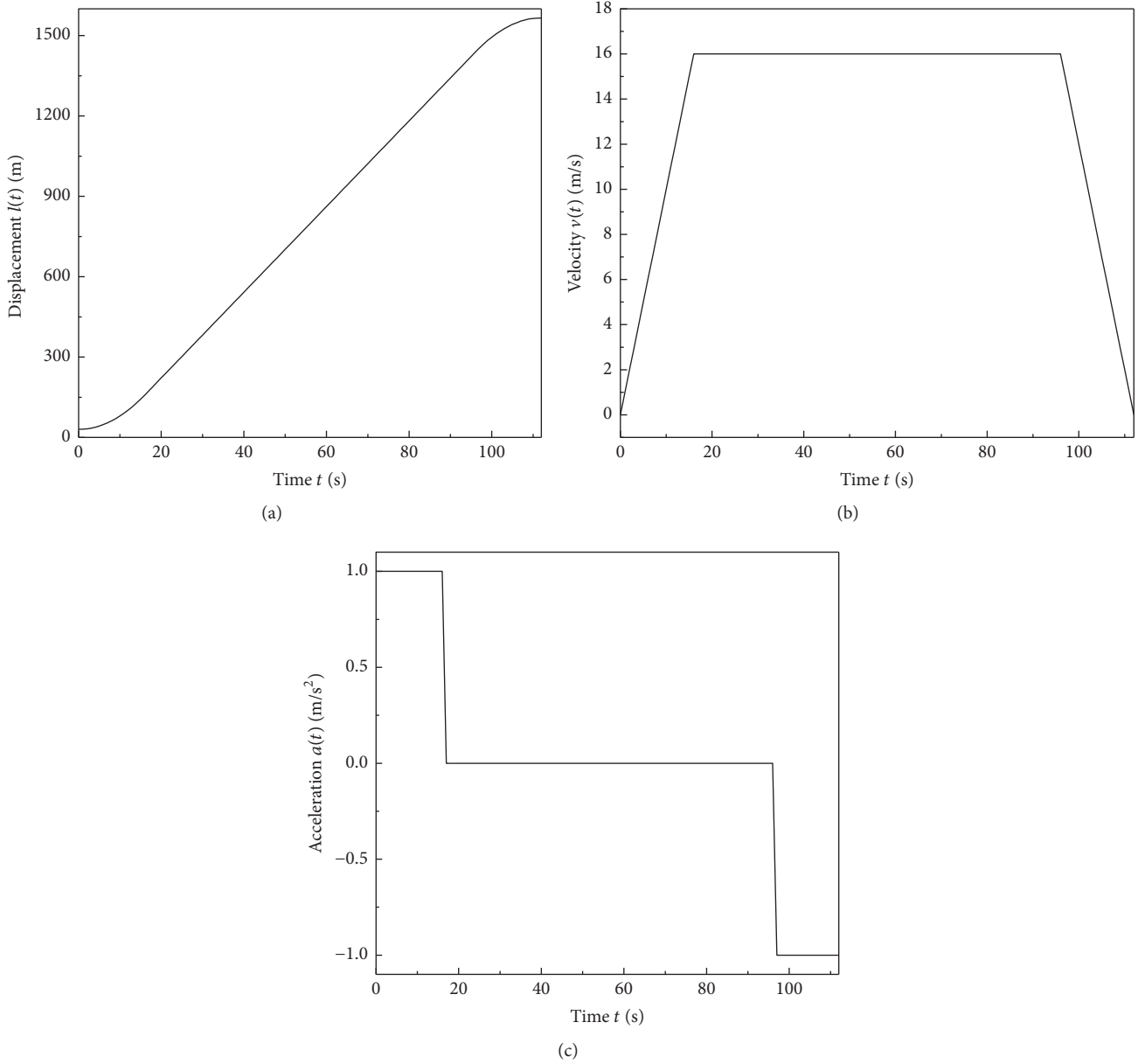
(a)

(b)

(c)

FIGURE 4: Prescribed movement profiles.

For the convenient of dealing with the constraint condition, the sequence of elements in $\mathbf{Q}$ is transformed, and the expression of $\mathbf{G}_0$ can be expressed as

$$\mathbf{G}_{01,4(2n)+2} = \mathbf{G}_{02,4(2n)+2} = -1,$$
$$\mathbf{G}_{03,4(2n)+3} = -\mathbf{G}_{03,4(2n)+4} = \frac{2}{d}. \tag{24}$$

The process of transforming DAEs to ODEs and obtaining the solution is the same as above, and it could be solved by Newmark-β method.

3. Results and Analysis

3.1. Parameters. In mine hoisting system, travelling distance ranges is large and continuously being increased. For example, in the South African gold mining industry, the depth of Kloof Gold Mine shaft is 2085 m, and the hoisting distance of South Deep Gold Mine has reached 3000 m. Now in China, new mines with shaft depths in the region of 1000–2000 m, based on parallel hoisting system, have recently been considered, for example, mine shafts in Chihong and Linyi. In this section, two-rope parallel hoisting system is discussed. The initial and maximum lengths of ropes are reset as 30 m and 1566 m, respectively. The downward movement profiles are shown in Figure 4.

TABLE 1: System parameters used in calculation.

Parameter	Value
ρ	11.5 kg/m
J	4.518×10^{-3} kg·m^2
Q_1^a, Q_2^a	1.746×10^8 N
Q_2^d, Q_2^d	1.227×10^4 N·m^2
$-Q_1^b, Q_2^b$	8.539×10^5 N·m
$-Q_1^c, Q_2^c$	7.969×10^5 N·m
ζ_u, ζ_θ	1.3×10^{-4}
d	0.35 m
m_c	20 t
J_{cx}	8.313×10^3 kg·m^2
J_{cz}	1.155×10^4 kg·m^2
k_c	8×10^5 N/m
c_c	6.7×10^4 Ns/m
r_1	1.1 m
r_2	0.8 m
R	2.5 m

Following the regulations that are mentioned above for parameter symbols, system parameters used in calculation are listed in Table 1, in which R is the radius of drum.

The longitudinal drive deviation $e_i(t)$ on ith rope could be denoted as

$$e_i(t) = es_i(t) + er_i(t), \quad i = 1, 2, \qquad (25)$$

where $es_1(t) = e_S \sin(n_1 \cdot (l(t) - l_0)/R)$ and $es_2(t) = e_S \sin(n_2 \cdot (l(t) - l_0)/R + \alpha)$ denote swing amplitude of noncircular drum, respectively. The e_S and α are expressed as $e_S = \kappa \cdot R$ and $\alpha = \varsigma \cdot \pi$, in which κ and ς are scale coefficients; in this paper, $\kappa = 0.001$ and $\varsigma = 0$. The coefficients n_1 and n_2 denote degree of defect distribution, respectively; in this paper, $n_1 = 1$ and $n_2 = 2$. $er_1(t) = 0$ and $er_2(t) = (e_r/R)(l(t) - l_0)$ denote relative deviation induced by radius' error of drum, respectively. The e_r is expressed as $e_r = \xi \cdot R$, in which ξ is a scale coefficient.

3.2. Dynamic Response under Drive Deviation.

The dynamic responses of the hoisting system are affected by many factors, but the influence of the radius' error of the hoisting rope e_r is more important because it brings large tension difference. In this paper, the following parametric study will concentrate on the influence of the radius' error of the hoisting rope e_r and the dynamic responses are investigated. In addition, the variable-domain finite element number $n = 5$ is used for the convergence of the solution, and the results are shown in Figures 5~8.

As shown in Figures 5~7, the tension and torsion of both ropes fluctuate greatly at the beginning because of hoisting acceleration, and the fluctuation decreases with the hoisting velocity at constant speed, but resonances occur while the natural frequency is close to the excitation frequency, which is shown in Figure 8. It is obvious that the longitudinal and torsional frequencies about hoisting ropes system decrease as the length increases, but the rotational frequencies about conveyance keep almost unchanged. Intersection points between
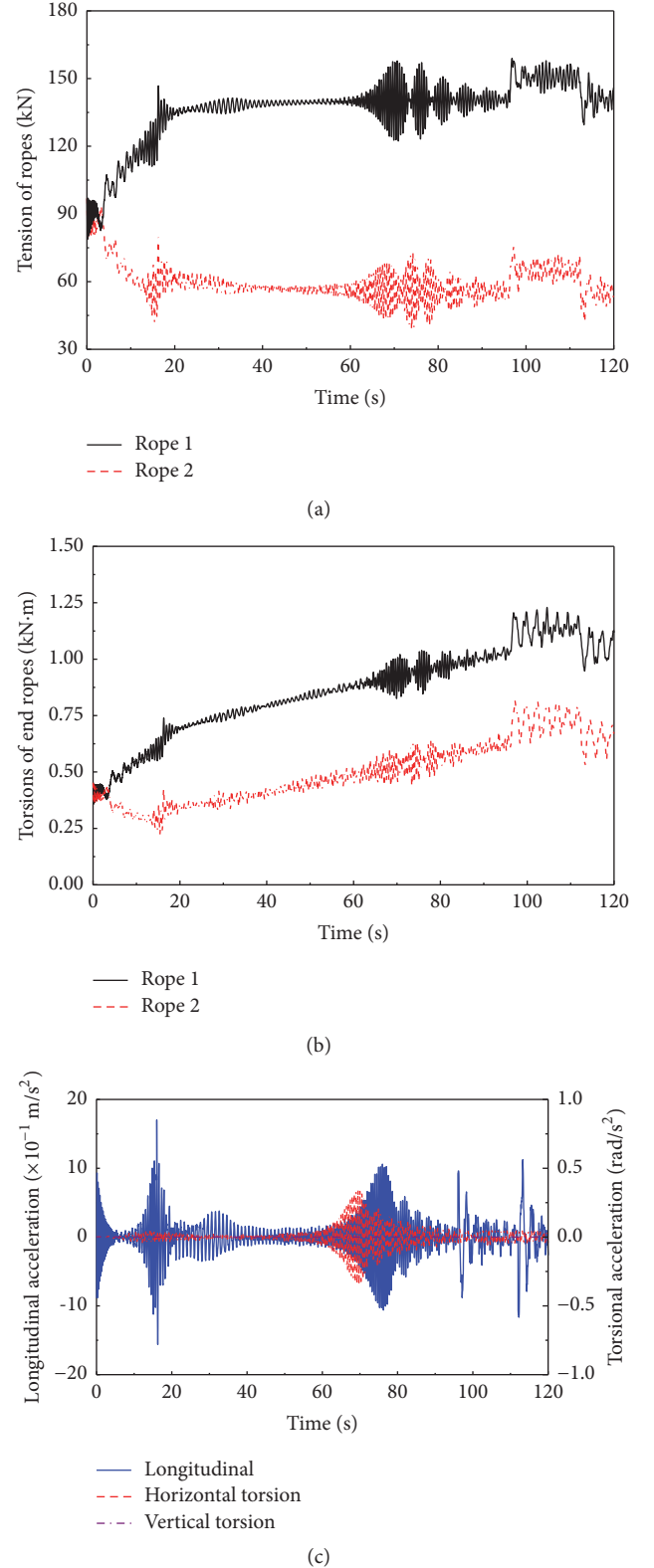

(a)

(b)

(c)

FIGURE 5: (a) Tensions, (b) torsions of the end ropes, and (c) accelerations of conveyance, calculated using $\xi = 0.0005$.

the natural frequencies and the excitation frequencies denote the resonance locations. It should be noted that there are
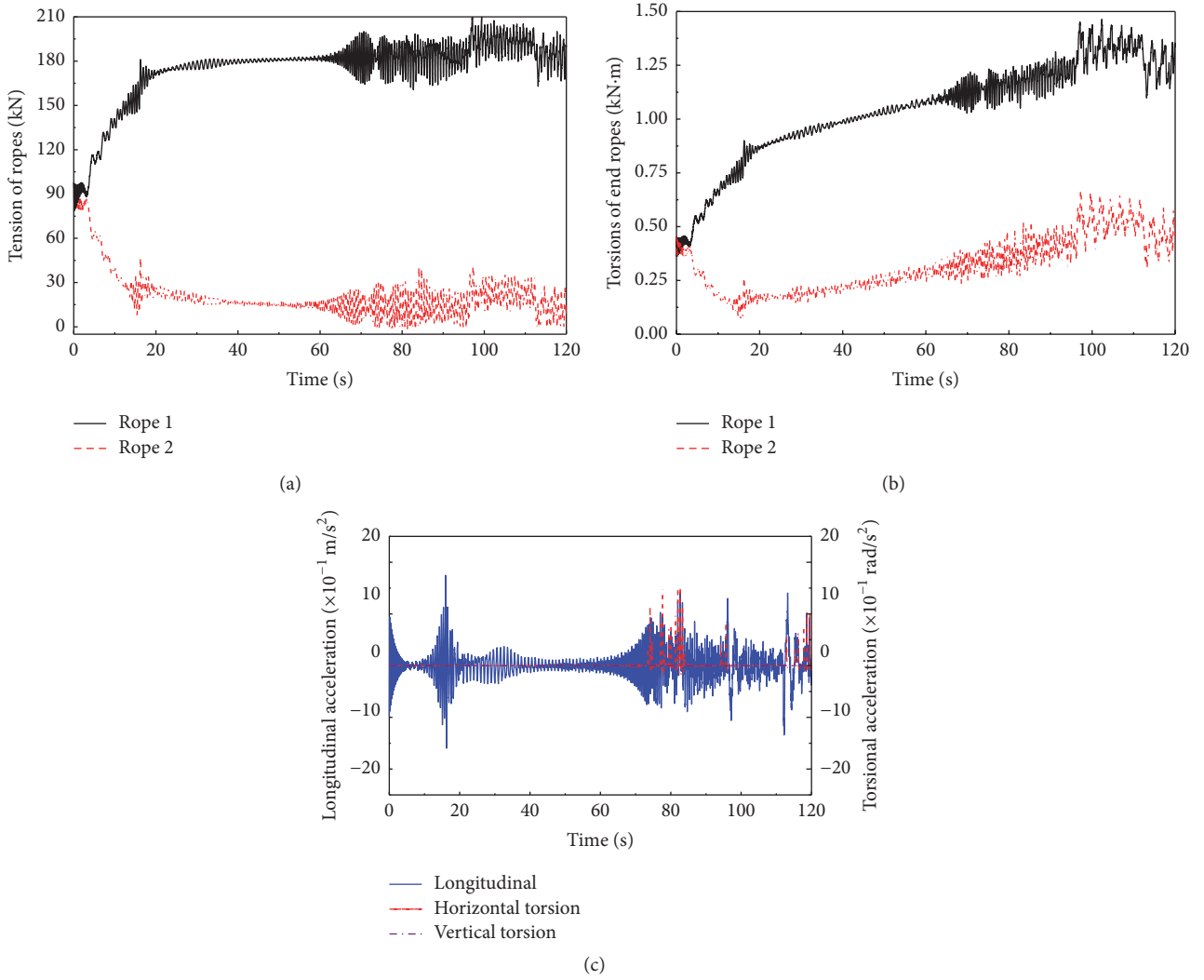
(a)

(b)

(c)

FIGURE 6: (a) Tensions, (b) torsions of the end ropes, and (c) accelerations of conveyance, calculated using $\xi = 0.001$.

multiple resonance locations during time interval 60~90 s, which validate the results of Figures 5~7. Although the torsion of ropes has approximately the same trend of vibration with tension in the beginning, there is some difference that the torsions of two ropes increase even if the tension of one rope drops gradually or the rope is slack. The reason for this phenomenon is that the weight of rope along varying length goes up and the tension of upper ends of rope rises gradually; therefore the torsions of the two ropes move up which also can be explained by (5) and (7). The accelerations of conveyance change violently in the horizontal direction during one rope alternating between the slack and tight states.

The dynamic tension difference between the ropes with the coefficient $\xi = 0.0015$ (Figure 7) is changed more than that with the coefficient $\xi = 0.001$ (Figure 6) and $\xi = 0.0005$ (Figure 5), which indicates that the deviation between ropes caused by the winding radius' error of drum can bring large influence to the tension difference. It is obvious that even if the deviation was only 1/1000 of the radius, the tension of one rope would dramatically drop, even close to zero, which

means that there is an obvious tension imbalance between two ropes. It is worth noting that intermittent tension of one rope would happen and last for a long time, which is shown in Figure 6(a), if the deviation (for example, 1/1000 of the radius) was inappropriate. It should be emphasized that unreasonable discordance between ropes would bring tension imbalance and should be controlled during the design and manufacture of drum, especially in super deep parallel hoisting system.

4. Conclusions

This paper addresses the modeling of parallel hoisting system considering the drive deviation, and the Vd-FEM and Lagrange's equations of the first kind are used to derive the equations of motion of the system. The dynamic model using Vd-FEM proposed for parallel hoisting system can be readily utilized to solve several challenging problems, including the slack or tight condition of ropes, the tensions and torsions between conveyance and ropes, and the rotation of the conveyance.
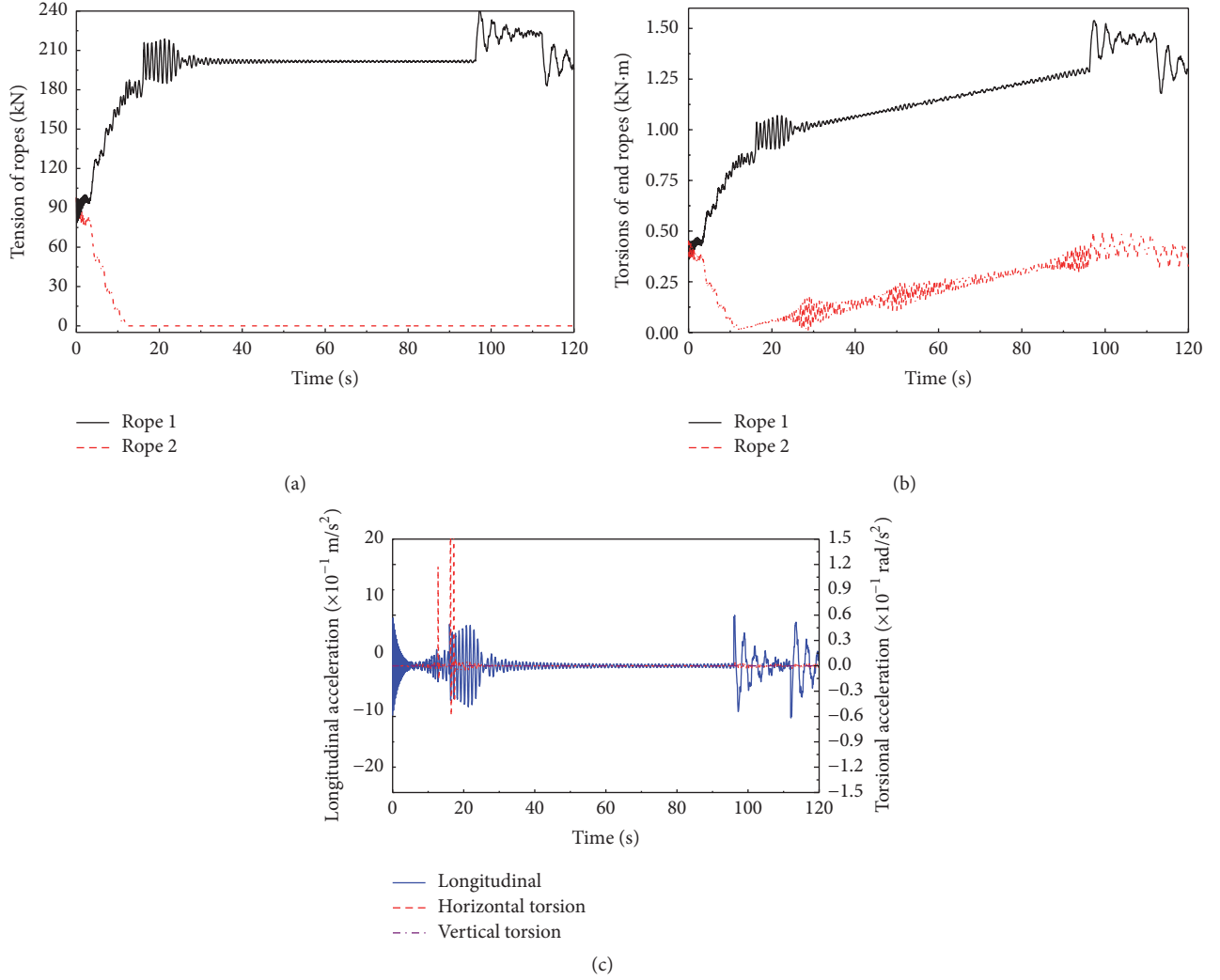
Rope 1
Rope 2

(a)

Rope 1
Rope 2

(b)

Longitudinal
Horizontal torsion
Vertical torsion

(c)

FIGURE 7: (a) Tensions, (b) torsions of the end ropes, and (c) accelerations of conveyance, calculated using $\xi = 0.0015$.

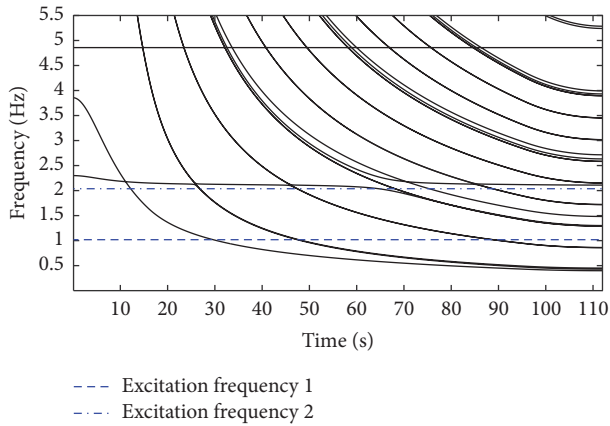Excitation frequency 1
Excitation frequency 2

FIGURE 8: Longitudinal, torsional, and excitation frequencies.

It should be noted that the torsions of two ropes increase even if the tension of one rope drops gradually or the rope is slack. The drive deviation (only 1/1000 of the radius) between ropes caused by the winding radius' error of drum will bring large influence to the tension difference and even lead to slack rope. And unreasonable discordance between ropes should be controlled for the design and manufacturing of drum on super deep parallel hoisting system.

Appendix

The matrix of element mass, damping, stiffness, and force is listed as follows:

$$\mathbf{m}_{i,j} = \rho \mathbf{A}_1,$$

$$\mathbf{c}_{i,j} = \rho \left(2\mathbf{A}_3 + 2v\mathbf{A}_2^T - v\mathbf{A}_2 \right) + \zeta_u Q_i^a \mathbf{A}_2^T + \kappa \rho v \mathbf{A}_{11},$$

$$\mathbf{k}_{ui,j}$$

$$= \rho \left(\mathbf{A}_6 + 2v\mathbf{A}_7 + a\mathbf{A}_2^T + v^2 \mathbf{A}_{14} - v^2 \mathbf{A}_4 - v\mathbf{A}_5 \right)$$

$$+ Q_i^a \mathbf{A}_4 + \zeta_u Q_i^a \mathbf{A}_7 + \kappa \left(\rho v \mathbf{A}_{12} + \rho v^2 \mathbf{A}_{13} \right),$$

$$\mathbf{c}_{ui\theta i,j} = \zeta_u Q_i^b \mathbf{A}_2^T,$$

$$\mathbf{k}_{ui\theta i,j} = 0.5 \left(Q_i^b + Q_i^c \right) \mathbf{A}_4 + \zeta_u Q_i^b \mathbf{A}_7,$$

$$\mathbf{f}_{ui,j}$$

$$= \rho v^2 \mathbf{A}_9 + \rho \left(g - a \right) \mathbf{A}_8 - \left(\rho g l + \frac{m_c g}{k} \right) \mathbf{A}_9$$

$$+ \rho g \mathbf{A}_{15} - \kappa \rho v^2 \mathbf{A}_{10},$$

$$\mathbf{m}_{\theta i,j} = J \mathbf{A}_1,$$

$$\mathbf{c}_{\theta i,j} = J \left(2\mathbf{A}_3 + 2v\mathbf{A}_2^T - v\mathbf{A}_2 \right) + \zeta_\theta Q_i^d \mathbf{A}_2^T + \kappa J v \mathbf{A}_{11},$$

$$\mathbf{k}_{\theta i,j}$$

$$= J \left(\mathbf{A}_6 + 2v\mathbf{A}_7 + a\mathbf{A}_2^T + v^2 \mathbf{A}_{20} - v^2 \mathbf{A}_4 - v\mathbf{A}_5 \right)$$

$$+ Q_i^d \mathbf{A}_4 + \zeta_\theta Q_i^d \mathbf{A}_7 + \kappa \left(J v \mathbf{A}_{12} + J v^2 \mathbf{A}_{13} \right),$$

$$\mathbf{c}_{\theta i u i,j} = \zeta_\theta Q_i^c \mathbf{A}_2^T,$$

$$\mathbf{k}_{\theta i u i,j} = 0.5 \left(Q_i^b + Q_i^c \right) \mathbf{A}_4 + \zeta_\theta Q_i^c \mathbf{A}_7,$$

$$\mathbf{f}_{\theta i,j} = \frac{\left[- \left(m_c/k + \rho l \right) g \mathbf{A}_9 + \rho g \mathbf{A}_{15} \right] Q_i^c}{Q_i^a},$$

$$\text{(A.1)}$$

where

$$\kappa = \begin{cases} 1, & j = n \\ 0, & \text{others.} \end{cases} \tag{A.2}$$

The matrixes of coefficients are as follows:

$$\mathbf{A}_1 = \int_{(j-1)l(t)/n}^{jl(t)/n} \mathbf{N}_j^T \mathbf{N}_j dx,$$

$$\mathbf{A}_2 = \int_{(j-1)l(t)/n}^{jl(t)/n} \mathbf{N}_{j,x}^T \mathbf{N}_j dx,$$

$$\mathbf{A}_3 = \int_{(j-1)l(t)/n}^{jl(t)/n} \mathbf{N}_j^T \mathbf{N}_{j,t} dx,$$

$$\mathbf{A}_4 = \int_{(j-1)l(t)/n}^{jl(t)/n} \mathbf{N}_{j,x}^T \mathbf{N}_{j,x} dx,$$

$$\mathbf{A}_5 = \int_{(j-1)l(t)/n}^{jl(t)/n} \mathbf{N}_{j,x}^T \mathbf{N}_{j,t} dx,$$

$$\mathbf{A}_6 = \int_{(j-1)l(t)/n}^{jl(t)/n} \mathbf{N}_j^T \mathbf{N}_{j,tt} dx,$$

$$\mathbf{A}_7 = \int_{(j-1)l(t)/n}^{jl(t)/n} \mathbf{N}_j^T \mathbf{N}_{j,tx} dx,$$

$$\mathbf{A}_8 = \int_{(j-1)l(t)/n}^{jl(t)/n} \mathbf{N}_j^T dx,$$

$$\mathbf{A}_9 = \int_{(j-1)l(t)/n}^{jl(t)/n} \mathbf{N}_{j,x}^T dx,$$

$$\mathbf{A}_{10} = \mathbf{N}_n^T \big|_{x=l(t)},$$

$$\mathbf{A}_{11} = \mathbf{N}_n^T \mathbf{N}_n \big|_{x=l(t)},$$

$$\mathbf{A}_{12} = \mathbf{N}_n^T \mathbf{N}_{n,t} \big|_{x=l(t)},$$

$$\mathbf{A}_{13} = \mathbf{N}_n^T \mathbf{N}_{n,x} \big|_{x=l(t)},$$

$$\mathbf{A}_{14} = \int_{(j-1)l(t)/n}^{jl(t)/n} \mathbf{N}_j^T \mathbf{N}_{j,xx} dx,$$

$$\mathbf{A}_{15} = \int_{(j-1)l(t)/n}^{jl(t)/n} x \mathbf{N}_{j,x}^T dx,$$

$$\text{(A.3)}$$

where the derivatives of shape function about t and x are given as

$$\mathbf{N}_{j,x} = \left[\frac{4n^2 x}{l^2} - \frac{n(4j-1)}{l} \quad \frac{4n(2j-1)}{l} - \frac{8n^2 x}{l^2} \quad \frac{4n^2 x}{l^2} - \frac{n(4j-3)}{l} \right],$$

$$\mathbf{N}_{j,xx} = \frac{4n^2}{l^2} \begin{bmatrix} 1 & -2 & 1 \end{bmatrix},$$

$$\mathbf{N}_{j,t} = \frac{vnx}{l^3} \left[(4j-1)l - 4nx \quad 8nx - 4(2j-1)l \quad (4j-3)l - 4nx \right],$$

$$\mathbf{N}_{j,xt} = \frac{nv}{l^3} \left[(4j-1)l - 8nx \quad 16nx - 4(2j-1)l \quad (4j-3)l - 8nx \right],$$

$$\mathbf{N}_{j,tt} = \frac{nx}{l^4} \begin{bmatrix} -l^2 a + 2lv^2 + 4l^2 aj - 8ljv^2 + 12nv^2 x - 4lanx \\ 4\left(l^2 a - 2lv^2 - 2l^2 aj + 4ljv^2 - 6nv^2 x + 2lanx \right) \\ \left(-3l^2 a + 6lv^2 + 4l^2 aj - 8ljv^2 + 12nv^2 x - 4lanx \right) \end{bmatrix}^T.$$

$$\text{(A.4)}$$

Competing Interests

Acknowledgments

References

[1] J. Du, H. Bao, C. Cui, and D. Yang, "Dynamic analysis of cable-driven parallel manipulators with time-varying cable lengths," *Finite Elements in Analysis and Design*, vol. 48, no. 1, pp. 1392–1399, 2012.

[2] W. D. Zhu and J. Ni, "Energetics and stability of translating media with an arbitrarily varying length," *Journal of Vibration and Acoustics, Transactions of the ASME*, vol. 122, no. 3, pp. 295–304, 2000.

[3] S. Kaczmarczyk and W. Ostachowicz, "Transient vibration phenomena in deep mine hoisting cables. Part 1: mathematical model," *Journal of Sound and Vibration*, vol. 262, no. 2, pp. 219–244, 2003.

[4] J. Wang, G. Cao, Z. Zhu, Y. Wang, and W. Peng, "Lateral response of cable-guided hoisting system with time-varying length: theoretical model and dynamics simulation verification," *Proceedings of the Institution of Mechanical Engineers Part C: Journal of Mechanical Engineering Science*, vol. 229, no. 16, pp. 2908–2920, 2015.

[5] W. D. Zhu and H. Ren, "An accurate spatial discretization and substructure method with application to moving elevator cable-car systems—part I: methodology," *Journal of Vibration and Acoustics, Transactions of the ASME*, vol. 135, no. 5, 10 pages, 2013.

[6] S. Kawamura, H. Kino, and C. Won, "High-speed manipulation by using parallel wire-driven robots," *Robotica*, vol. 18, no. 1, pp. 13–21, 2000.

[7] E. Ottaviano, "Analysis and design of a four-cable-driven parallel manipulator for planar and spatial tasks," *Proceedings of the Institution of Mechanical Engineers, Part C: Journal of Mechanical Engineering Science*, vol. 222, no. 8, pp. 1583–1592, 2008.

[8] B. Y. Duan, Y. Y. Qiu, F. S. Zhang, and B. Zi, "On design and experiment of the feed cable-suspended structure for super antenna," *Mechatronics*, vol. 19, no. 4, pp. 503–509, 2009.

[9] M. H. Korayem and M. Bamdad, "Dynamic load-carrying capacity of cable-suspended parallel manipulators," *The International Journal of Advanced Manufacturing Technology*, vol. 44, no. 7-8, pp. 829–840, 2009.

[10] X.-G. Shao, Z.-C. Zhu, Q.-G. Wang, P. C. Chen, B. Zi, and G.-H. Cao, "Non-smooth dynamical analysis and experimental validation of the cable-suspended parallel manipulator," *Proceedings of the Institution of Mechanical Engineers, Part C: Journal of Mechanical Engineering Science*, vol. 226, no. 10, pp. 2456–2466, 2012.

[11] Y. Wang, G. Cao, Z. Zhu, J. Wang, and N. Wang, "1483. Longitudinal response of parallel hoisting system with time-varying rope length," *Journal of Vibroengineering*, vol. 16, no. 8, pp. 4088–4101, 2014.

[12] O. C. Zienkiewicz and R. L. Taylor, *The Finite Element Method for Solid and Structural Mechanics*, Butterworth-Heinemann, 2005.

[13] L. Meirovitch, *Principles and Techniques of Vibrations*, Prentice Hall, Upper Saddle River, NJ, USA, 1997.

[14] M. Stylianou and B. Tabarrok, "Finite element analysis of an axially moving beam, part I: time integration," *Journal of Sound and Vibration*, vol. 178, no. 4, pp. 433–453, 1994.

[15] M. Stylianou and B. Tabarrok, "Finite element analysis of an axially moving beam, part II: stability analysis," *Journal of Sound and Vibration*, vol. 178, no. 4, pp. 455–481, 1994.

[16] P.-H. Wang, R.-F. Fung, and M.-J. Lee, "Finite element analysis of a three-dimensional underwater cable with time-dependent length," *Journal of Sound and Vibration*, vol. 209, no. 2, pp. 223–249, 1998.

[17] K. A. F. Moustafa, E. H. Gad, A. M. A. El-Moneer, and M. I. S. Ismail, "Modelling and control of overhead cranes with flexible variable-length cable by finite element method," *Transactions of the Institute of Measurement and Control*, vol. 27, no. 1, pp. 1–20, 2005.

[18] G. A. Costello, *Theory of Wire Rope*, Springer Science & Business Media, Berlin, Germany, 1997.

[19] J. M. Hamilton, "Vibration-based techniques for measuring the elastic properties of ropes and the added mass of submerged objects," *Journal of Atmospheric and Oceanic Technology*, vol. 17, no. 5, pp. 688–697, 2000.

[20] S. K. Soltakhanov, M. P. Yushkov, and S. A. Zegzhda, *Mechanics of Non-Holonomic Systems: A New Class of Control Systems*, Foundations of Engineering Mechanics, Springer Science & Business Media, Berlin, Germany, 2009.